Nonlinear Model of High-Speed Solar Wind Streams

A. J. HUNDHAUSEN

High Altitude Observatory, National Center for Atmospheric Research
Boulder, Colorado 80302

A hydrodynamic model describing the generation and propagation of high-speed plasma streams in the solar wind is presented. The model is based upon numerical integrations of the conservation equations for a time-dependent, spherically symmetric, radial flow of interplanetary plasma. The nearly radial nature of the solar wind flow justifies the use of the model to approximate 'corotating streams,' e.g., nonspherically symmetric flows that are steady in a frame of reference rotating with the sun. The predicted variations in solar wind properties are in good agreement with those observed at 1 AU for a reasonable choice of parameters characterizing a 'coronal disturbance' at the heliocentric distance of 28 R_S. This choice must include a perturbation of the coronal temperature but need not include perturbations of the coronal density or mass efflux. The streams produced by such a disturbance 'steepen' in transit to the orbit of the earth, with formation of a pair of shocks predicted at slightly larger heliocentric distances. The average dependencies of density and temperature upon the solar wind speed deduced from the model resemble those inferred from solar wind observations. This suggests that the major density changes associated with high-speed streams are the products of interplanetary compression and rarefaction within the evolving stream structure. The same processes explain the deviations of proton temperature from their average dependence on solar wind speed; however, that basic dependence appears to reflect the temperature changes imposed on the plasma in the corona.

The existence of long-lived high-speed solar wind streams was established by the observations performed on the Mariner 2 space probe in 1962 [*Snyder et al.*, 1963; *Neugebauer and Snyder*, 1966]. The apparent tendency of the observed streams to recur at approximately the 27-day solar rotation period suggested their interpretation as a spatially structured flow pattern, nearly steady in a frame of reference rotating with the sun, but swept past a stationary observer by solar rotation. Such 'solar corpuscular beams' had, in fact, been inferred and discussed before the advent of direct solar wind observations from 27-day recurrences in geomagnetic activity [e.g., *Chapman*, 1964].

The high-speed streams observed by Mariner 2 displayed a fairly consistent pattern of correlated variations in solar wind properties: a rapid rise, followed by a slower decline, in the solar wind speed; a short interval of very high densities near the leading edge of the speed elevation, followed by a longer interval of abnormally low densities; a general elevation of proton temperatures with a fast rise, slow decline profile similar to that of the flow speed [*Snyder and Neugebauer*, 1964; *Neugebauer and Snyder*, 1966]. These variations were interpreted by the Mariner 2 experimenters in terms of a fluid interaction between solar wind streams with different expansion speeds. For example, the overtaking of low-speed plasma by the high-speed stream would be expected to produce a compression (and the observed high densities) near the leading edge of the resulting interaction region. This same interpretation was also presented and expanded upon by several others. *Parker* [1963] and *Sarabhai* [1963] pointed out that a rarefaction (and the observed low densities) would be expected on the declining portion of the speed elevation. *Dessler and Fejer* [1963] and *Dessler* [1967] predicted an 'eastward' (i.e., in the same sense as solar rotation) deflection of plasma near the leading edge of the stream, followed by a 'westward' deflection.

Quantitative models of the fluid interaction invoked above have been formulated only recently. *Carovillano and Siscoe* [1969] analyzed the interaction of 'corotating' (i.e., steady in a frame rotating with the sun) plasma streams in the solar equatorial plane on the basis of linearized fluid equations, valid for small ampli-

tude deviations from a steady, spherically symmetric background of solar wind. *Siscoe and Finley* [1969, 1970, 1972] and *Hirose et al.* [1970] have continued this analysis for more general boundary conditions. These models give quantitative confirmation (within the limitation of the small-amplitude assumption) to the qualitative conclusions regarding stream interactions that were cited above. *Siscoe* [1970] derived approximate analytic solutions for the nonlinear development of corotating solar wind streams (or filaments) sufficiently 'thin' not to disturb the flow of the surrounding solar wind. Very recently, two papers have described solutions to the full nonlinear fluid equations (with attention again restricted to the solar equatorial plane). In one of these *Goldstein* [1971] has integrated the hydrodynamic equations beyond 10 R_S under the assumption of boundary conditions (and solutions) periodic in solar longitude. The numerical procedures used by Goldstein did not permit carrying the solutions farther from the sun than $\sim$150 R_S ($\sim$¾ AU), where steep density gradients developed. *Matsuda and Sakurai* [1972] have integrated the magnetohydrodynamic equations between ⅓ and 1 AU under the assumption of a small nonradial velocity component.

This paper will describe another attempt to analyze the interaction of corotating plasma streams. Solutions to the nonlinear hydrodynamic equations will be derived for transient, spherically symmetric flows. Under an assumption very similar to that of Matsuda and Sakurai, that of small nonradial velocities, these solutions will be shown to approximate those describing corotating streams in the solar equatorial plane. The new contributions to be set forth here are: (1) the capability of the present analysis to include hydrodynamic discontinuities, in particular the formation of shocks at steep gradients; (2) the resulting ability to extend the solutions to larger heliocentric distances than were previously considered; (3) a suggested interpretation of several observed statistical correlations among solar wind parameters in terms of the fluid interactions between streams.

THEORETICAL MODEL

The formulation of a quantitative solar wind model requires simultaneous solution of the appropriate mass, momentum, and energy conservation equations for the expanding coronal plasma. The inherent nonlinearity of these equations, the complexity of the forces and energy sources that enter into them, and the presence of the time t and vector position $\mathbf{r}$ (relative to the center of the sun) as independent variables all contribute to the difficulty of solution. Much attention has been given to the formulation of models under the assumption of a steady, spherically symmetric flow. This simplification reduces the conservation equations to ordinary differential equations in the single independent variable r, the heliocentric distance, and permits treatment of numerous physical forces and energy sources (see *Hundhausen* [1972], for a review). In contrast, any model of the interaction of solar wind streams must include consideration of either time or the vector position as independent variables, ruling out any such convenient simplification. A much less sophisticated physical approach becomes necessary in obtaining solutions of the resulting system of partial differential equations. Some of the forces and energy sources that have been successfully incorporated into the steady, spherically symmetric models and found to be of some significance must be neglected to yield a tractable problem.

Thus our present model will involve a large number of simplifying assumptions. The solar wind plasma will be assumed to consist of completely ionized hydrogen, affected only by the forces due to the pressure gradient and solar gravity; thus all magnetic effects are neglected. The flow of plasma will be assumed to be adiabatic; thus thermal conduction and any dissipation of wave energy have been neglected. If attention is restricted to the solar equatorial plane and all effects due to motions normal to that plane are neglected, the equations of mass, radial momentum, azimuthal momentum, and energy conservation become:

$$\frac{\partial \rho}{\partial t} + \frac{1}{r^2}\frac{\partial}{\partial r} r^2 \rho u_r + \frac{1}{r}\frac{\partial}{\partial \phi}(\rho u_\phi) = 0 \qquad (1)$$

$$\rho \frac{\partial u_r}{\partial t} + \rho u_r \frac{\partial u_r}{\partial r} + \rho u_\phi \frac{1}{r}\frac{\partial u_r}{\partial \phi} - \rho \frac{u_\phi^2}{r} = -\frac{\partial P}{\partial r} - \rho \frac{GM_S}{r^2} \qquad (2)$$

$$\rho \frac{\partial u_\phi}{\partial t} + \rho u_r \frac{\partial u_\phi}{\partial r} + \rho u_\phi \frac{1}{r} \frac{\partial u_\phi}{\partial \phi} + \rho \frac{u_\phi u_r}{r} = -\frac{1}{r} \frac{\partial P}{\partial \phi} \quad (3)$$

$$\frac{\partial}{\partial t} (P\rho^{-\gamma}) + u_r \frac{\partial}{\partial r} (P\rho^{-\gamma}) + u_\phi \frac{1}{r} \frac{\partial}{\partial \phi} (P\rho^{-\gamma}) = 0 \quad (4)$$

where

- t is the time.
- r is heliocentric distance.
- ϕ is solar longitude.
- ρ is the mass density.
- u_r is the radial velocity component.
- u_ϕ is the azimuthal velocity component.
- P is the pressure.
- G is the gravitational constant.
- M_S is the mass of the sun.
- γ is the ratio of specific heats.

These are essentially the same equations (based on the same assumptions) used in other models of solar wind stream interactions. Choice of γ as the ratio of specific heats corresponds to our adiabatic assumption; use of an arbitrary value would correspond to the polytropic flow assumed in the other models. *Siscoe and Finley* [1970, 1972] also considered motions out of the solar equatorial plane, while *Matsuda and Sakurai* [1972] have also included the magnetic force in their momentum equations. Solutions to (1) to (4) that correspond to corotating structures (i.e., steady flows in a frame of reference rotating with the sun) would be functions purely of r and $\eta = \phi - \omega t$, where η is the solar longitude in the frame rotating with the angular speed ω of the sun.

An additional simplifying assumption. The propagation of transient, spherically symmetric disturbances in the solar wind has been the subject of numerous quantitative analyses (see the review by *Hundhausen* [1970]). *Simon and Axford* [1966] have argued that the plasma flow in such disturbances should be similar in its basic features, if not in detail, to that in corotating streams. *Burlaga et al.* [1971] have applied this analogy to actual observations. In fact, a quantitative argument for the analogy can be given and can be used to demonstrate that the difference between the conservation laws describing the two flows is actually of the order $|u_\phi/u_r|$. As this ratio is observed to be small in the solar wind at 1 AU and is probably small throughout the coronal expansion, the interaction and flow of corotating plasma streams can be approximated by proper application of the well-developed techniques for computing time-dependent, spherically symmetric flows.

Consider the conservation laws for mass, radial momentum, and energy, as in (1), (2), and (4). Each of these conservation equations contains two 'divergence' terms that reflect the gain or loss of the conserved quantity from a differential volume element due to the radial and azimuthal velocities; each term is linear in the appropriate velocity component. The ratios of the azimuthal and radial divergence terms in the three equations are:

$$\frac{1}{r} \frac{\partial}{\partial \phi} (\rho u_\phi) \Big/ \frac{1}{r^2} \frac{\partial}{\partial r} (r^2 \rho u_r) \quad (5)$$

$$u_\phi \frac{1}{r} \frac{\partial u_r}{\partial \phi} \Big/ u_r \frac{\partial u_r}{\partial r} \quad (6)$$

$$u_\phi \frac{1}{r} \frac{\partial}{\partial \phi} (P\rho^{-\gamma}) / u_r \frac{\partial}{\partial r} (P\rho^{-\gamma}) \quad (7)$$

It is expected from the theory of the coronal expansion and verified by satellite observations near 1 AU that the solar wind flows almost radially from the sun, or $|u_\phi| \ll |u_r|$. Under this condition we might expect that the ratios 5, 6, and 7 are small and that the azimuthal divergences could be neglected in the conservation laws 1, 2, and 4. As the term $-\rho u_\phi^2/r$ in (2) is also negligible for $|u_\phi| \ll |u_r|$, equations 1, 2, and 4 can then be approximated by

$$\frac{\partial \rho}{\partial t} + \frac{1}{r^2} \frac{\partial}{\partial r} (r^2 \rho u_r) = 0 \quad (8)$$

$$\rho \frac{\partial u_r}{\partial t} + \rho u_r \frac{\partial u_r}{\partial r} = -\frac{\partial P}{\partial r} - \rho \frac{GM_S}{r^2} \quad (9)$$

$$\frac{\partial}{\partial t} (P\rho^{-\gamma}) + u_r \frac{\partial}{\partial r} (P\rho^{-\gamma}) = 0 \quad (10)$$

These are precisely the mass, momentum, and energy conservation laws for a transient, spherically symmetric, radial plasma flow.

The magnitude of the ratios 5, 6, and 7 can be estimated by recalling that corotating plasma

streams (and any interaction regions between them) should be nearly aligned with the spiral interplanetary magnetic field [e.g., *Parker*, 1963; *Dessler and Fejer*, 1963; *Colburn and Sonett*, 1966; *Belcher and Davis*, 1971; *Goldstein*, 1971; *Hundhausen*, 1972*a*, *b*]. This implies nearly equal azimuthal and radial gradients of any structure associated with the streams near 1 AU (where the average magnetic field spiral is at 45° to the radial); for example,

$$\left|\frac{1}{r}\frac{\partial u_r}{\partial \phi}\right| \approx \left|\frac{\partial u_r}{\partial r}\right|$$

Thus the ratios 5, 6, and 7 are nearly equal to $|u_\phi/u_r|$ at 1 AU. It is well established observationally that the flow of the solar wind is almost radial near the earth; e.g., the average value of $|u_\phi/u_r|$ inferred from the two years of spacecraft observations summarized by *Hundhausen et al.* [1970] is about 0.05, while the maximum excursion in $|u_\phi/u_r|$ within prominent high-speed streams discussed by *Siscoe* [1972] and *Gosling et al.* [1972] is ~0.1. Thus (8), (9), and (10) approximate (1), (2), and (4) to an accuracy of 10% at 1 AU. (A similar argument could be used to justify the neglect in writing equations 1–4 of the divergence terms due to flow out of the solar equatorial plane.)

For heliocentric distances other than 1 AU, estimation of the ratios 5, 6, and 7 requires some information regarding the variations with heliocentric distance of the relevant gradients and velocity components. The expected alignment of corotating streams with the spiral magnetic field lines implies that the ratios of azimuthal to radial gradients will vary approximately as $1/r$. The azimuthal velocity variations associated with the interaction of streams (the deflections mentioned earlier) are expected to grow with heliocentric distance near the sun (as an azimuthal pressure gradient develops) and to decline at large heliocentric distances (as the gradient becomes increasingly radial). Existing models of solar wind streams confirm this behavior of the azimuthal velocity. *Carovillano and Siscoe* [1969] find a nearly linear growth of u_ϕ with heliocentric distance, while *Siscoe and Finley* [1970] confirm this behavior near the sun but find a leveling off at 1 AU. *Matsuda and Sakurai* [1972], in their nonlinear analysis, find a more rapid increase in u_ϕ within 1 AU than in the above linearized (small perturbation) treatments of solar wind streams. As u_r changes only slowly with heliocentric distance beyond the 'critical point' [*Parker*, 1963] in the coronal expansion, the following can be expected:

1. For $r > 1$ AU, $|u_\phi/u_r|$ will increase only slowly, or probably decrease with increasing r. As the ratio of azimuthal to radial gradients varies approximately as $1/r$, the ratios 5, 6, and 7 should decrease slowly with increasing heliocentric distance.

2. For $r < 1$ AU, $|u_\phi/u_r|$ varies more rapidly than in proportion to r. As the ratio of azimuthal to radial gradients varies approximately as $1/r$, the ratios 5, 6, and 7 should decrease with decreasing heliocentric distance.

These conclusions are consistent with the quantitative predictions of the *Siscoe* [1970] model of thin solar wind filaments.

It thus appears that the ratios 5, 6, and 7 reach maximum values somewhere near 1 AU and are smaller both nearer the sun (but beyond ~0.05 AU) and at large heliocentric distances. As these ratios were estimated above to be only ~0.10 at 1 AU, we are led to the conclusion that the mass, radial momentum, and energy equations 1, 2, and 4 can be approximated by the simpler system 8, 9, and 10 with an accuracy of ~10%.

This conclusion justifies the analogy between the basic features of transient, spherically symmetric disturbances and corotating streams and allows us to use solutions for the former flow as a reasonable approximation to the latter. In following this course, we obtain no information regarding the azimuthal velocity component, as the azimuthal momentum equation has been dropped from the system. The behavior of this important indicator of corotating streams can be studied only in a more complete analysis. The flow pattern for the corotating stream, with fluid parameters as functions of r, t, and ϕ, is obtained from the spherically symmetric flow pattern, with fluid parameters as a function of r and t only, by attributing the time dependence at a given longitude ϕ to the rotation of a spatial structure, or by equating ϕ to $\eta_0 + \omega t$, where η_0 is a fixed position in a frame rotating with the sun. This is equivalent to the requirement that corotating solutions be functions only of $\eta = \phi - \omega t$. At a given position in a stationary frame of reference, the temporal variations

are, in either case, given simply by the solution in r and t. Only the 'phase' of the variation (the time associated with arrival of a particular fluid parcel at a given distance) changes at different solar longitudes.

Method of solution. We will employ here solutions to (8), (9), and (10) for transient spherically symmetric flow obtained by the numerical integration technique described by *Hundhausen and Gentry* [1969*a*, *b*]. In this technique an 'ambient' solar wind state is established by specification of the fluid parameters ρ, u_r, and P at two heliocentric positions r_1 and r_2. In the computations to be described below, r_1 was taken to be 0.133 AU (28 R_S) and r_2 to be 2.67 astronomical units. Fluid parameters were chosen to give a steady, adiabatic, supersonic solar wind in the shell between these two radii, with a number density of 7.5 cm^{-3}, a solar wind speed of 325 km sec^{-1}, and a pressure of 8.3×10^{-11} dyne cm^{-2} at 1 AU. These particular (and entirely typical) solar wind properties were chosen to facilitate a forthcoming comparison with actual observations. Such an adiabatic flow cannot be extended back toward the sun to less than ~0.1 AU; this fact largely dictated the choice of the inner boundary r_1. At a time defined to be $t = 0$, a prescribed temporal variation is imposed upon the fluid parameters $\rho(r_1, t)$, $u(r_1, t)$ and $P(r_1, t)$ at the 'inner boundary' $r = r_1$. The propagation of the resulting transient in the solar wind flow is then followed through the shell $r_1 \leq r < r_2$ by the numerical integration scheme.

PROPERTIES OF THE SOLUTIONS

As an illustration of the solutions obtained by this method, consider a specific example. Let the density $\rho(r_1, t)$ and the expansion speed $u(r_1, t)$ at the inner boundary maintain the constant values ρ_{1a} and u_{1a}. Let the pressure $P(r_1, t)$ increase linearly with time (beginning at $t = 0$) until the maximum value P_{1max} is attained at $t = \tau$, decrease linearly with the same rate to reattain the value P_{1a} at $t = 2\tau$, and remain at the latter value for $t > 2\tau$ (see Figure 1). This transient pressure pulse is completely described by specification of the amplitude parameter $\Pi \chi P_{1max}/P_{1a}$ and the duration parameter τ. The corresponding 'corotating' boundary condition involves a steady high-pressure region extending over solar longitudes (in a frame rotating with the sun) between η_0 and $\eta - 2\omega\tau$, with the maximum pressure at $\eta_0 - \omega\tau$.

Figures 2, 3, and 4 show the computed functions $u(r, t)$, $n(r, t)$, where n is the number density, and $P(r, t)$ at $t = 0$ (i.e., the ambient solar wind state) and at five later times. Figure 5 also shows a temperature $T(r, t)$ at the same times. T has been defined by the equation of state

$$P = 2(\rho/m)kT \qquad (11)$$

where m is the combined mass of a proton and an electron, and k is the Boltzmann constant. T is literally the average of the proton and electron temperatures. Comparison of the predicted T with an observed proton temperature (discussed later) requires the assumption that the temperatures of the protons and electrons be equal, or that the solar wind be described by a one-fluid model. In describing the solution displayed in Figures 2–5, we will use the terminology appropriate to a pure temporal evolution. In the approximation advocated above, this same terminology applies to the rotation of a steady spatial structure through a given solar longitude (in a stationary frame).

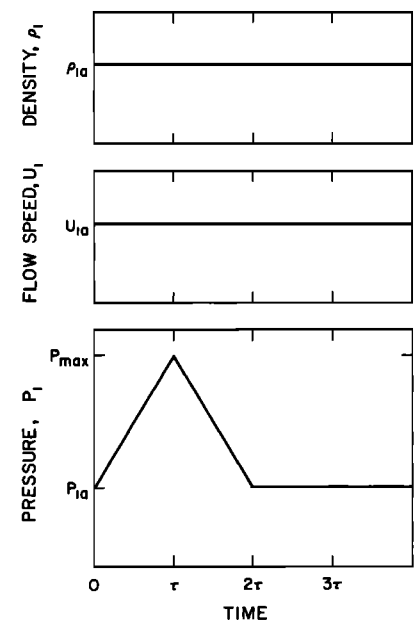

Fig. 1. The temporal variations in density, expansion speed, and pressure at $r_1 = 0.133$ AU. In the context of a 'one-fluid' model, this represents a variation only in the temperature.

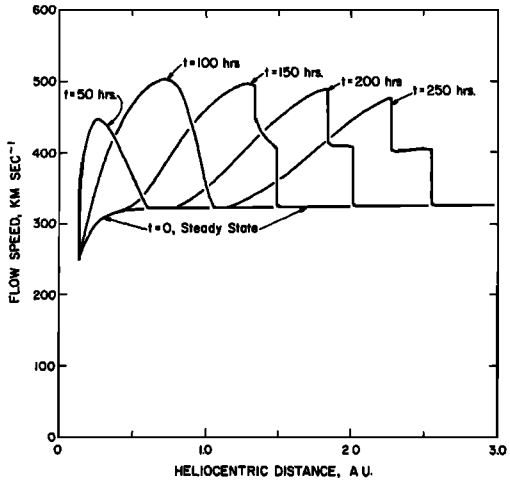

Fig. 2. The flow speed versus heliocentric distance given by the present model at six different times. The $t = 0$ curve shows the steady, adiabatic flow into which the high-speed stream propagates.

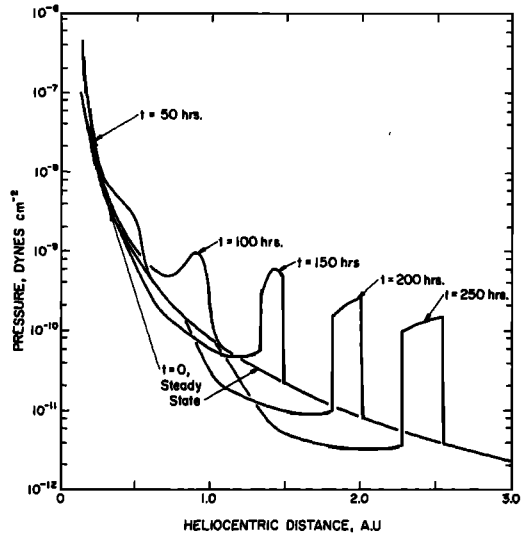

Fig. 4. The pressure versus heliocentric distance given by the present model at six different times.

The solar wind transient shown in Figures 2–5 is produced by the introduction of the transient pressure pulse at $r = r_1 = 0.133$ AU and the subsequent acceleration of plasma flowing from the sun. At $t = 50$ hours, when the maximum pressure is reached at r_1 for this particular case, all the plasma in the shell $r_1 < r \lesssim 0.60$ AU is moving faster than in the ambient flow (Figure 2). Between the outer edge of this shell and the position of maximum expansion speed, $r = 0.26$ AU, faster-moving plasma (at smaller heliocentric distances) is overtaking slower-moving plasma (at larger heliocentric distances). Thus the plasma in this region is being compressed, raising the density above the ambient profile (Figure 3). Between $r = r_1$ and $r = 0.26$ AU, faster-moving plasma

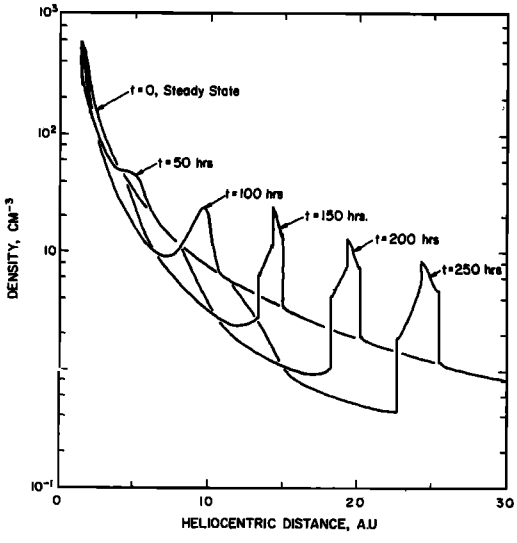

Fig. 3. The number density versus heliocentric distance given by the present model at six different times.

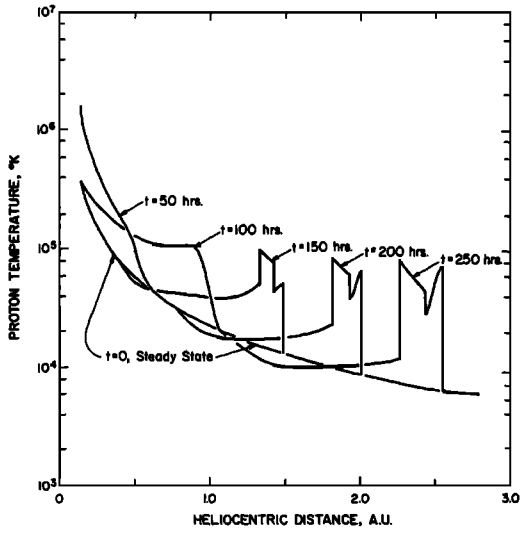

Fig. 5. The temperature versus heliocentric distance given by the present model at six different times.

(at larger heliocentric distances) is running away from slower-moving plasma (at smaller heliocentric distances). Thus the plasma in this region is being expanded, lowering the density below the ambient profile. The density structure shown in Figure 3 is entirely due to this compression-rarefaction effect beyond $r = r_1$. The pressure and temperature profiles (Figures 3 and 4) stem both from this adiabatic compression and expansion of the plasma and from the changes in the initial values (at $r = r_1$) of P and T for all the plasma that has passed through the inner boundary since $t = 0$.

The acceleration produced by the elevated pressure at $r = r_1$ continues until the ambient pressure is resumed at $t = 100$ hours. The maximum local expansion speed of 503 km sec^{-1} is reached at $r = 0.60$ AU and $t = 90.5$ hours. With the return to the ambient pressure for $t > 100$ hours the overall acceleration terminates; the fast-moving solar wind in the shell $r_1 < r \lesssim 1.05$ AU of Figure 2 subsequently 'coasts' outward into the ambient flow, continuing the compression and expansion processes described above. The fast plasma is continually (but gradually) decelerated as it sweeps up the slowly moving 'ambient material' in its path.

For $t > 100$ hours, the evolution of the solar wind transient is dominated by nonlinear steepening of the flow speed profile (Figure 2), or 'high-speed wave,' developed during the earlier acceleration. For example, between $t = 100$ and 150 hours, the front edge of the flow speed elevation has moved from 1.05 to 1.50 AU, the crest of the wave has moved from 0.71 to 1.29 AU, and the trailing edge of the elevation has moved only from 0.1 to ~0.4 AU. This relative motion of front, crest, and trailing edge of the high-speed wave distorts it into the sawtooth form evident in Figure 2. The continuing compression and rarefaction processes lead to the thin shell of very high densities ($1.32 < r < 1.50$ AU at $t = 150$ hours) near the front of the wave and the broad shell of low densities in the rest of the wave (Figure 3). These processes continue to influence the pressure and temperature signals of Figures 4 and 5. By $t = 150$ hours, the steepening of the wave profile has become sufficiently extreme to produce forward and reverse shock fronts [*Colburn and Sonett*, 1966] at the front and rear edges of the density compression. For $t > 150$ hours, this pattern of evolution continues. Note that the deceleration of the high-speed plasma is a relatively minor effect; the maximum flow speed within the wave decreases only from 502 km sec^{-1} at $t = 100$ hours to 477 km sec^{-1} at $t = 250$ hours.

Let us reiterate that the dynamical evolution described above applies, in the approximation discussed earlier, to corotating spatial structures, as well as to actual transients; solar longitude simply replaces time (as given above) as the parameter giving the state of evolution. To emphasize this point, note that the profiles of fluid parameters shown in Figures 2–5 at different times are equivalent to the profiles at different solar longitudes (in a frame of reference rotating with the sun). The corotating spatial structure corresponding to the solution described above is obtained by replacing the time t with the solar longitude (in a frame rotating with the sun) $\eta = \eta_0 - \omega t$. The dependences on heliocentric distance displayed at 50-hour time intervals in Figures 2–5 apply, for example, at 29.5-deg longitude intervals (for a solar rotation period of 25.4 days [*Allen*, 1955]). Figure 6 illustrates some of the characteristics of this spatial structure by means of a contour map of the radial expansion speed $u_r(r, \eta)$. Contour lines are given for $u_r = 335$ km sec^{-1}, just above the ambient expansion speed of 325 km sec^{-1}, and for $u_r = 475$ km sec^{-1}, near the maximum speed in the wave. Thus these contours identify the leading and trailing edges and the crest of

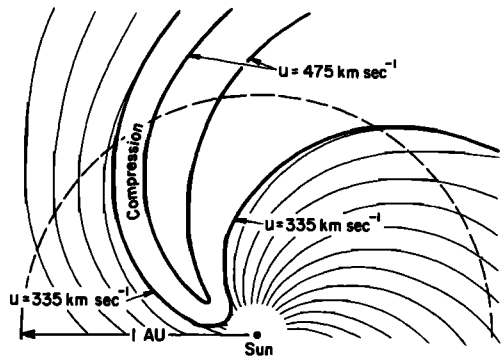

Fig. 6. The steady corotating high-speed structure equivalent to the transient solution of Figures 2–5. The contours at $u_r = 325$ and 475 km sec^{-1} indicate the extremities and peak of the high-speed stream. The light spiral lines are the streamlines in the ambient flow (in a frame of reference rotating with the sun).

the high-speed wave. The light spiral lines represent the streamlines in the ambient solar wind (the plasma has an azimuthal velocity component $u_\phi = -\omega r$ in this rotating frame of reference), or, alternatively, the lines of magnetic force drawn out from the sun by the solar wind. The high-pressure region at $r_1 = 0.133$ AU occupies 60° of longitude beginning at the arrow denoting 1 AU to the left of the sun. The formation of a localized high-speed wave, the advance of the crest of the wave relative to the leading and trailing edges (producing a compression and rarefaction), and the flow of ambient plasma into the leading edge of the wave are all apparent in Figure 6.

Comparison with other models. The solution described above exhibits the basic characteristics expected on the basis of the qualitative physical arguments summarized earlier. The differences between this solution and the models of small perturbations derived by *Carovillano and Siscoe* [1969] and by *Siscoe and Finley* [1969, 1972] are those that would be expected in the nonlinear development of such perturbations. Precise comparisons with the nonlinear models of *Goldstein* [1971] and of *Matsuda and Sakurai* [1972] are difficult because of the small differences in physical assumptions (e.g., the use of polytropic indices of 1.5 and 1.2 in these two models) and boundary conditions employed therein. Nonetheless, the general characteristic of the solutions obtained in this and the other two nonlinear analyses are very similar. The only significant differences arise in the region of large compression where the numerical integration technique used by Goldstein breaks down, where the viscous dissipation and magnetic forces included by Matsuda and Sakurai have their largest effects, and where the neglect of azimuthal divergence terms in the present model is least valid.

Comparison with observations. The model of high-speed solar wind streams developed above will be used to discuss several stream-related solar wind phenomena. Before the discussion is entered, some assurance that the model predicts stream characteristics in reasonable agreement with those actually observed in the solar wind would be reassuring. A high-speed stream observed between April 21 and 27, 1966, by the twin Vela 3 spacecraft [*Bame et al.*, 1971] has been selected for comparison with the model; this selection was made on the basis of the availability of observations and the apparent simplicity of this particular stream. Hourly averages of the observed solar wind speed u, proton number density n (where $n = \rho/m$), and proton temperature T are shown as functions of time in Figure 7. The high-speed stream is taken to begin with the simultaneous increases in u and n late on April 21; the pre-stream solar wind conditions are then $u = 325$ km sec^{-1}, $n = 7.5$ cm^{-3}, and $T = 4 \times 10^4$ °K. These are the same values used to define the ambient solar wind used in the model. The variations $u(r_e, t)$, $n(r_e, t)$, $T(r_e, t)$ predicted at $r_e = 1$ AU by the solution of Figures 2–5 are shown in Figure 7 by the dark lines. These predictions do agree reasonably well with the observations. In truth, the parameters Π and τ for the solution were selected to give such agreement; the fact that reasonable agreement can be obtained for all three observed quantities, using a two-parameter set of solutions, gives some justification for using this model in the forthcoming discussions. This justification is limited; for a more extensive comparison of the model with high-speed stream observations leading to a broader justification for use of the model, see *Gosling et al.* [1972].

SHOCK FORMATION IN HIGH-SPEED SOLAR WIND STREAMS

The possibility of shock formation in corotating high-speed solar wind streams has long been

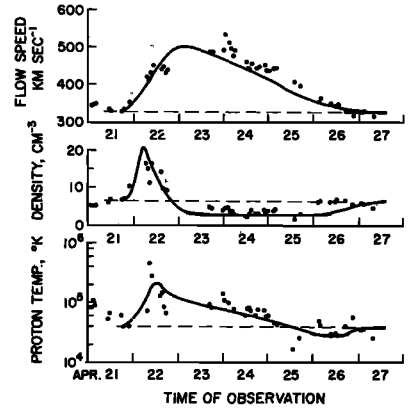

Fig. 7. A comparison of the flow speed, density, and temperature variations predicted at 1 AU by the present model with the variations observed by the Vela 3 spacecraft in an actual solar wind stream.

recognized [e.g., *Sturrock and Spreiter*, 1965; *Sonett and Colburn*, 1965; *Dessler and Fejer*, 1963; *Colburn and Sonett*, 1966]. In the interaction of a high-speed stream with a slower-moving ambient plasma under consideration here, a pair of shocks, propagating away from and toward the sun relative to the plasma, would be expected to bound the region of compressed plasma at an advanced stage in the nonlinear evolution of the stream. The solution displayed in Figures 2–5 does indeed show the formation of such a shock pair. As this phenomenon has not been quantitatively included in the other models of high-speed plasma streams, some further discussion is in order.

This discussion should, however, be prefaced by specific warnings about two limitations inherent in the present model. The first of these concerns the neglect of all but the radial divergence terms in the mass, radial momentum, and energy conservation laws. In essence, such an approximation ignores any deflection of ambient plasma by an overtaking high-speed stream and should lead to an overestimate of the resulting compression. The predicted time (or heliocentric distance) of shock formation should then be an underestimate. The neglect of azimuthal divergence terms has been explicitly described; it should also be recognized that restriction of (1) to (4) to the solar equatorial plane implicitly neglects 'latitudinal' divergence terms. The second warning concerns the ability of the numerical integration scheme used here to proceed through the steep gradients (infinite in the absence of dissipative terms in the fluid equations) at any shock front. This ability derives from the use of an 'artificial viscosity term' [*Hundhausen and Gentry*, 1969*a*, *b*] that serves to spread the shock over a finite width; the strength of the viscous term is taken not from physical considerations but from the requirement that the resulting shock width be smaller than other characteristic dimensions of the flow pattern, yet larger than the mesh size used in the numerical integrations. This 'smearing' of any shock front introduces an inherent uncertainty as to its position and, for very weak shocks, its very existence. Both of these difficulties will lead us to qualify any quantitative conclusions regarding shock formation.

A detailed examination of the particular solution described and displayed in Figures 2–5 indicates that the pair of shock fronts form between $t = 100$ and $t = 111$ hours. If the shocks are present before the earlier time, they are too weak to be discerned in the numerical solution; they are distinctly discernible at the later time. The forward shock appears to form at a heliocentric distance between 1.04 and 1.15 AU, whereas the reverse shock appears to form between 0.96 and 1.04 AU. The spatial configurations of the shock fronts are shown in Figure 8, superposed on the overall stream structure of Figure 7. The heavy lines show the shock fronts, and the dashed segments near 1 AU illustrate the uncertainties as to the positions of shock formation. The parameters Π and τ describing the initial pressure pulse at $r = r_1$ were chosen to give temporal variations at 1 AU that resembled a particular set of observations (Figure 7). The absence of any visible shocks in those observations (weak shocks might have escaped undetected, and moderate-strength shocks could have occurred in the gaps in the data) influenced their choice. Selection of larger values of Π or shorter values of τ would lead to formation of the shock pair within $r = 1$ AU.

Although the existence of corotating shocks has been inferred from recurrent geomagnetic sudden commencements and the first shock wave observed in the solar wind may have been associated with a corotating high-speed stream, it is generally held that most of the high-speed plasma streams observed in the solar wind are not accompanied by corotating shocks [*Ogilvie*, 1972; *Hundhausen*, 1972*a*]. The single example of the present model shown above indicates that a reasonable boundary condition near the sun can be selected to give a predicted stream

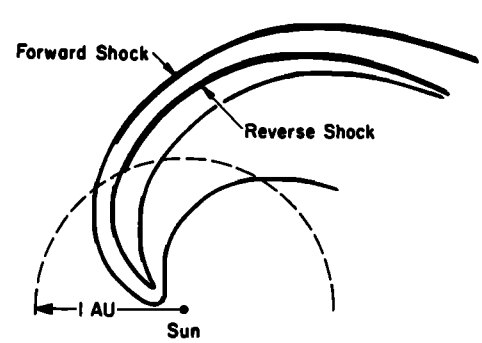

Fig. 8. The spatial configuration of the forward and reverse shock fronts that form in the corotating stream of Figure 6.

structure at 1 AU that resembles the observed structure, and, in particular, has not led to shock formation within that heliocentric distance. However, the evolution of the stream is so rapid near 1 AU that shock formation occurs shortly thereafter. This conclusion is verified by solutions involving other choices of the parameters Π and τ; it appears that corotating shock pairs should form rapidly in the high-speed plasma streams observed near 1 AU and should be a common feature of the interplanetary plasma at large heliocentric distances. While the predicted position of shock formation in a particular stream is probably underestimated owing to the neglect of azimuthal and latitudinal motions, the rate of steepening indicated by the present model is so rapid near 1 AU that only a gross breakdown of our assumptions could negate this conclusion.

One further prediction regarding shock formation is of some interest. As was illustrated by the example of Figures 2–5, the forward and reverse shocks tend to form at nearly the same time (or solar longitude) in the evolution of the stream structure. Thus the reverse shock appears at a smaller heliocentric distance than does the forward shock. It is, in fact, not too difficult to select Π and τ such that the forward shock has not formed when the leading edge of a high-speed stream passes 1 AU, but the reverse shock is formed within 1 AU. In other words, an observer at 1 AU might well observe a high-speed stream with a reverse shock but no forward shock. *Burlaga* [1970] has, in fact, reported the observation of a reverse shock located well within the rising speed portion of a solar wind stream, but found no preceding forward shock. *Ogilvie* [1972] has argued that this reverse shock was corotating. The present model offers an interpretation of this observation in terms of the rapidly evolving structure in a high-speed stream.

High-Speed Solar Wind Streams and Correlated Variations of Solar Wind Parameters

It is well known [e.g., *Hundhausen et al.*, 1970; *Burlaga and Ogilvie*, 1970*a*, *b*; *Ness et al.*, 1971] that most observed solar wind parameters undergo large variations. Further, the variations in different parameters do not occur randomly but are, in many cases, correlated. The best known of these correlations involve an inverse statistical relationship between solar wind density and speed [*Neugebauer and Snyder*, 1966; *Hundhausen et al.*, 1970; *Burlaga and Ogilvie*, 1970*b*; *Mihalov and Wolfe*, 1971] and a direct statistical relationship between proton temperature and solar wind speed [*Strong et al.*, 1966; *Hundhausen et al.*, 1967, 1970; *Burlaga and Ogilvie*, 1970*a*]. Among other such observed correlations is a statistical relationship between flow direction and solar wind speed [*Coon*, 1968; *Siscoe et al.*, 1969; *Hundhausen et al.*, 1970].

The physical interpretation of these correlations has been the topic of several discussions. *Burlaga and Ogilvie* [1970*a*] have emphasized the significance of the proton temperature–flow speed relationship and posed its explanation as a test of a complete solar wind theory. This suggestion was pursued by *Hartle and Barnes* [1970], who have interpreted the average proton temperature versus flow speed observations of Burlaga and Ogilvie as defining 'a continuum of average macroscopic states of the solar wind . . .' and have attempted its explanation in terms of a sequence of steady, spherically symmetric coronal expansion models. The members of the sequence differ from one another in the details of an assumed proton heating function operative between 2 and $\sim$20 R_s; the predicted proton temperatures and expansion speeds at 1 AU can be made to match the observed relationship of *Burlaga and Ogilvie* [1970*a*] for expansion speeds less than about 400 km sec^{-1}. *Barnes et al.* [1971] have proposed a further refinement of this 'extended heating' concept in which a variable flux of hydromagnetic waves passing through the corona beyond 2 R_s leads to a sequence of models with a direct relationship between proton temperature and expansion speed at 1 AU. The density–flow speed relationship has been discussed less; most coronal expansion models, in fact, predict too high an interplanetary density (unless a coronal density lower than that generally accepted is assumed) at any flow speed. However, *Parker* [1965] has called attention to the difficulty in explaining the low solar wind densities prevailing in high-speed streams on the basis of the expansion of a 'conduction corona,' and partially based the hypothesis of an extended heating of the coronal plasma (as adopted by Hartle and

Barnes and by Barnes, Hartle, and Bredekamp) on this argument. *Belcher* [1971] and *Alazraki and Conturier* [1971] have advocated substantial acceleration of the coronal plasma by Alfvén wave pressure on similar logical grounds.

In all the above-mentioned discussions, the correlations among solar wind parameters have been interpreted in terms of physical processes occurring in a steady, spherically symmetric coronal expansion. A possible alternative explanation of the observed statistical relationships among solar wind parameters is that they result from averaging over the correlated variations implicit in solar wind structures related to either spatial inhomogeneities or transient changes in the expanding corona [*Hundhausen*, 1970, 1972*b*]. In particular, the correlation of flow direction and flow speed has generally been interpreted in this manner [*Siscoe et al.*, 1969; *Carovillano and Siscoe*, 1969]. The model of high-speed plasma streams described above permits further consideration of this alternative. The justification for using the model, with all its limitations and oversimplifications, in such a discussion stems from its ability to predict variations in solar wind parameters at 1 AU that closely resemble those in observed solar wind streams (e.g., Figure 7 or *Gosling et al.* [1972]).

Consider first the predicted densities and flow speeds displayed as functions of time in Figure 7. It should be recalled that the density variation in this example is entirely the result of an interplanetary compression and rarefaction of the solar wind plasma; no density or flux variation was introduced at the inner boundary in initiating this stream (Figure 1). The resulting prediction of low densities at high flow speeds (a condition prevailing throughout the rarefaction) is precisely that combination of parameters difficult to explain on the basis of steady spherically symmetric coronal expansion models and thus the source of some puzzlement [*Parker*, 1965; *Belcher*, 1971]. Suppose that the predicted density variations of Figure 7 are used to compute a time-averaged density $\langle n \rangle$ in various speed intervals, and thus to predict a relationship between $\langle n \rangle$ and u implicit in the stream structure. For any given speed interval u to $u + \Delta u$, where u is above the ambient flow speed, both high density values from the compression region and low density values from the rarefaction region enter into the averaging process. At high speeds, the latter receive greater weight in a time average because of the slow change in speed within the rarefaction, and the average density $\langle n \rangle$ is found to be lower than the ambient density. At speeds just above the ambient level, the very large densities found in the compression region overcome this tendency, and the average density $\langle n \rangle$ is found to be somewhat larger than the ambient density. The resulting inverse dependence of $\langle n \rangle$ upon u is qualitatively consistent with the observed statistical relationship between the same two solar wind properties. A quantitative comparison between prediction and observation would require computation of $\langle n \rangle$-u relationships for high-speed streams with different amplitudes and durations and a superposition of these relationships for the distribution of amplitudes and durations that actually occurs in the solar wind. Such a superposition cannot be performed at the present time, as this distribution remains undetermined. The distribution of wave amplitudes and durations might even change with time (e.g., through a cycle of solar activity); different average densities and somewhat different dependences of $\langle n \rangle$ upon u have been reported from different sets of observations [*Neugebauer and Snyder*, 1966; *Hundhausen et al.*, 1970; *Burlaga and Ogilvie*, 1970*b*] and could be the effect of changes in stream structure. However, one further prediction of the present model might provide a simple test of this proposed interpretation of the $\langle n \rangle$-u relationship. If the variability in the solar wind density is strongly related to the occurrence of interplanetary compressions and rarefactions, the density should be strongly correlated with the observed time derivative of the flow speed. This correlation would be expected to be more fundamental than the known $\langle n \rangle$-u relationship.

Consider next the predicted proton temperatures and flow speeds displayed as functions of time in Figure 7. The temperature variation at 1 AU might be the result of both interplanetary changes (related to the adiabatic compression and rarefaction of the plasma) and the temperature changes imposed on the plasma at the inner boundary (Figure 1). The separation of these two possible influences will be central to any interpretation of the observed relationship between proton temperature and flow speed

in terms of the present model of high-speed streams.

Suppose that the predicted temperature variations of Figure 7 are used to compute a time-averaged proton temperature $\langle T \rangle$ in various speed intervals and thus to predict a relationship between $\langle T \rangle$ and u implicit in the stream structure. Figure 9 shows the line traced out in flow speed–temperature coordinates by the variations in these two parameters, and will aid both in visualizing the averaging process and in understanding the result. The predicted speed-temperature state of the plasma proceeds in a clockwise sense around the closed curve on Figure 9 at the variable rate indicated by the time markings. The highest temperatures occur on the short-lived rising portion of the speed variation (the compression); lower but generally above-ambient temperatures occur on the long-lived declining portion of the speed variation (the rarefaction). In any above ambient speed interval, these high- and low-temperature branches of the trace are averaged together, weighted by the time spent in that interval on each branch, in computing $\langle T \rangle$. The resulting $\langle T \rangle$-u relationship is shown in Figure 9 by the dashed line. As might be expected in the light of the general high level of temperatures throughout the flow speed elevation, a direct dependence of $\langle T \rangle$ upon u is predicted.

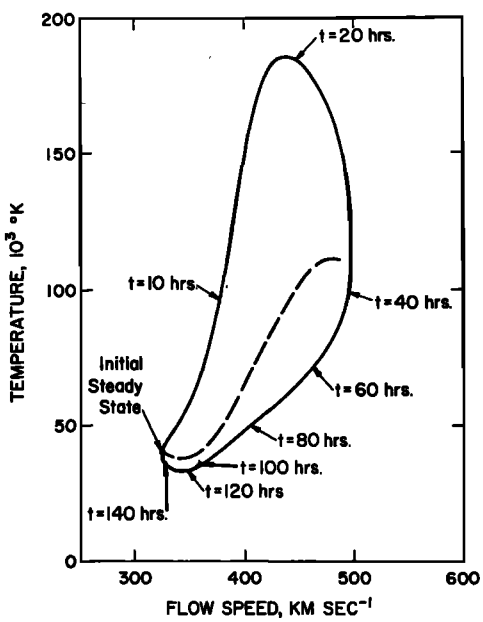

Fig. 9. The trace of flow speed versus temperatures predicted at 1 AU by the solutions in Figures 2–5. Temporal motion around the closed curve is indicated by the time markings. The dashed curve shows the average temperature as a function of flow speed inferred from the model.

It should be recalled that the $\langle T \rangle$-u relationship shown in Figure 9 is based on a single example. Computations performed with different choices of Π and τ, giving streams with different amplitudes and durations at 1 AU, yield a trace of speed-temperature states similar in shape to that of Figure 9. Waves with large-amplitude, highly steepened speed profiles show higher temperatures on the upper branch and lower temperatures on the lower branch of the trace than do streams with small-amplitude more symmetric speed profiles. Nonetheless, the $\langle T \rangle$-u relationships deduced from examples with reasonable amplitudes and durations (at 1 AU) all are very close to that shown in Figure 9. For example, Figure 10 adds the $\langle T \rangle$-u relationship from an example with a peak speed of 700 km sec^{-1} and a duration of 220 hours (the dashed line) to that of Figure 9 (the solid line). We can thus conclude that the superposition of $\langle T \rangle$-u relationships for any realistic distribution of stream amplitudes and durations must give a final predicted $\langle T \rangle$-u relationship close to that inferred by combining the two examples in Figure 10.

The dots in Figure 10 show the average proton temperatures observed in 25 km sec^{-1} speed intervals by Vela 3 spacecraft between 1965 and 1967 [*Hundhausen et al.*, 1970]. The predicted relationship between temperature and flow speed (with an implicit one-fluid assumption) agrees reasonably well with the observations; the two predicted curves generally fall below the observed points by 25–30%. This difference could be lessened (or possibly eliminated) either by choosing a higher temperature in the ambient solar wind or by moving the inner boundary of the model to a larger heliocentric distance. In view of the approximate nature of the model, any such change would tell us little more than can be deduced from Figure 10, that the model of high-speed streams can predict a temperature-speed relationship similar to that actually observed. Hence it is entirely reasonable to interpret the observed relationship as the result of averaging through

the organized temperature and speed variations found in high-speed plasma streams.

If this interpretation is accepted, the problem of separating the effects of interplanetary and inner boundary changes becomes central to further physical understanding. The dotted line on Figure 10 connects the speed-temperature states that would result at 1 AU from a sequence of steady solutions to (8)–(10) using the boundary conditions given in Figure 1. In other words, since no spatial or temporal variations are considered in the derivation of this line, it represents the solar wind states expected at 1 AU under the same physical assumptions made in our model, but in the absence of any effects related to the interaction of solar wind streams with different expansion speeds. It would, in fact, be expected that as $\tau \rightarrow \infty$ in the stream model, the latter effects would become progressively weaker and the trace of speed-temperature states in a stream would approach this line of steady adiabatic solar wind states. The dotted line can then be interpreted as the result of the temperature changes imposed on the plasma at the inner boundary. The deviations in the trace of states (Figure 9) given by the present model from the dotted line of Figure 10 are attributable to the interplanetary processes of compressional heating and expansive cooling.

Further examination of Figure 10 reveals a close correspondence between the $\langle T \rangle$-u relationship deduced from two examples of our stream model and the trace of adiabatic steady states; the former curves (solid and dashed) show a slightly faster rise of $\langle T \rangle$ with u than the latter curve (dotted). It thus appears that the effects of compressional heating and expansive cooling nearly compensate for one another when averaged through an entire stream. This might be expected in a small-amplitude wave, but need not hold for a large-amplitude structure. In particular, a high-speed stream propagating into a slow-moving background must be decelerated, so that some kinetic energy of the stream converts to the thermal energy of the interaction region. This effect is probably responsible for the difference between the $\langle T \rangle$-u relationships predicted by the stream models and the steady adiabatic states in Figure 10. The small size of this difference indicates that the conversion of kinetic to thermal energy occurs slowly; this interpretation is consistent with the very gradual deceleration of the stream shown in Figure 2.

Our understanding of the correlated speed and temperature variations predicted by the present stream model and their implications regarding the observed correlation of solar wind temperature and speed can be summarized as follows. The direct dependence of $\langle T \rangle$ upon u deduced from the model is nearly the same for all streams with reasonable amplitudes and durations and is similar to that expected from a sequence of steady, adiabatic solar wind states. The latter similarity indicates that the $\langle T \rangle$-u relationship can be largely attributed to the temperature changes at the inner boundary (i.e, the corona). This same conclusion has been drawn from purely empirical evidence by *Burlaga and Ogilvie* [1973]. Note that if no temperature change were imposed as a boundary condition (as, for example, by *Matsuda and Sakurai* [1972]), $\langle T \rangle$ would depend only weakly upon u as a result of the slow conversion of

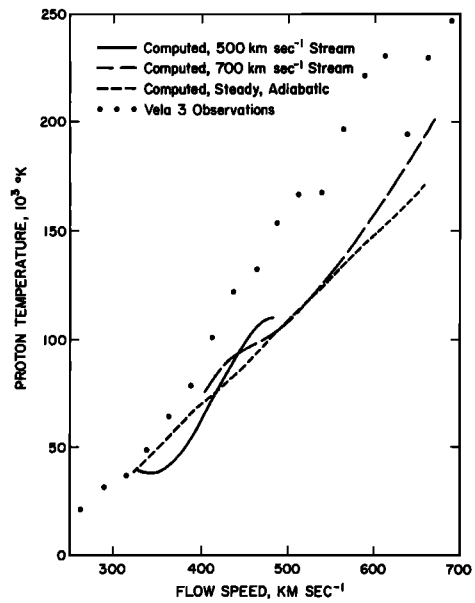

Fig. 10. The average temperature as a function of flow speed computed from: (1) the solution of Figures 2–5 (solid line); (2) a solution in which the maximum speed is 700 km sec^{-1} (dashed line); (3) a steady adiabatic expansion at each 'inner boundary' state of Figure 1 (dotted line). The dots show the average proton temperatures observed in 25 km sec^{-1} speed intervals by the Vela 3 spacecraft.

kinetic energy to thermal energy. The observed direct and strong dependence of $\langle T \rangle$ on u thus implies that a coronal temperature variation must be present at the source of high-speed solar wind streams. In the present model this variation has to be assumed to occur at 28 R_s; this location should not be taken as physically significant, as it was chosen as the 'inner boundary' purely to permit use of an adiabatic flow assumption and neglect of azimuthal divergence terms. In contrast, the predicted deviations of the speed-temperature state in a stream from the average temperature-speed relationship are largely the effects of compressional heating and expansive cooling in interplanetary space. The size of these deviations depends strongly on amplitude and duration of the stream and would be present even if no temperature variation were present at the source of the stream.

Acknowledgments. My thanks go to Dr. R. A. Gentry and Mrs. J. V. Young for their contributions to the development and execution of the numerical computations described in this paper and to S. J. Bame for permission to use the unpublished Vela 3 data of Figure 7. Valuable discussions were held with Drs. L. F. Burlaga, J. T. Gosling, and M. D. Montgomery; Dr. T. M. Holzer has made valuable comments on the manuscript.

The National Center for Atmospheric Research is sponsored by the National Science Foundation.

* * *

The Editor thanks L. F. Burlaga and G. L. Siscoe for their assistance in evaluating this paper.

REFERENCES

Alazraki, G., and P. Conturier, Solar wind acceleration caused by the gradient of Alfvén wave pressure, *Astron. Astrophys., 13,* 380, 1971.

Allen, C. W., *Astrophysical Quantities,* Athlone, London, 1955.

Bame, S. J., J. R. Asbridge, H. E. Felthauser, H. E. Gilbert, A. J. Hundhausen, D. M. Smith, I. B. Strong, and S. J. Sydoriak, A Compilation of Vela 3 Solar Wind Observations, 1965 to 1967, *Rep. LA-4536,* vol. 1, Los Alamos Sci. Lab., Los Alamos, N. Mex., 1971.

Barnes, A., R. E. Hartle, and J. H. Bredekamp, On the energy transport in stellar winds, *Astrophys. J.,* L53, 1971.

Belcher, J. W., Alfvenic wave pressures and the solar wind, *Astrophys. J., 168,* 509, 1971.

Belcher, J. W., and L. Davis, Jr., Large amplitude Alfvén waves in the interplanetary medium, 2, *J. Geophys. Res., 76,* 3534, 1971.

Burlaga, L. F., A reverse hydromagnetic shock in the solar wind, *Cosmic Electrodynamics, 1,* 233, 1970.

Burlaga, L. F., and K. W. Ogilvie, Heating of the solar wind, *Astrophys. J., 159,* 659, 1970*a*.

Burlaga, L. F., and K. W. Ogilvie, Magnetic and thermal pressures in the solar wind, *Solar Phys., 15,* 61, 1970*b*.

Burlaga, L. F., and K. W. Ogilvie, Solar wind temperature and speed, *J. Geophys. Res., 78,* in press, 1973.

Burlaga, L. F., K. W. Ogilvie, D. H. Fairfield, M. D. Montgomery, and S. J. Bame, Energy transfer at colliding streams in the solar wind, *Astrophys. J., 164,* 137, 1971.

Carovillano, R. L., and G. L. Siscoe, Corotating structure in the solar wind, *Solar Phys., 8,* 401, 1969.

Chapman, Sydney, *Solar Plasma, Geomagnetism, and Aurora,* Gordon and Breach, New York, 1964.

Colburn, D. S., and C. D. Sonett, Discontinuities in the solar wind, *Space Sci. Rev., 5,* 439, 1966.

Coon, J., Solar wind observations, in *Earth's Particles and Fields,* edited by B. M. McCormac, p. 359, Reinhold, New York, 1968.

Dessler, A. J., Solar wind and interplanetary magnetic field, *Rev. Geophys. Space Phys., 5,* 1, 1967.

Dessler, A. J., and J. A. Fejer, Interpretation of K_p index and M-region geomagnetic storms, *Planet. Space Sci., 11,* 505, 1963.

Goldstein, B., Nonlinear corotating solar wind structure, submitted to *J. Geophys. Res.,* 1971.

Gosling, J. T., A. J. Hundhausen, V. Pizzo, and J. R. Asbridge, Compressions and rarefactions in the solar wind: Vela 3, *J. Geophys. Res., 77,* 5442, 1972.

Hartle, R. E., and A. Barnes, Nonthermal heating in the two-fluid solar wind model, *J. Geophys. Res., 75,* 6915, 1970.

Hirose, T., M. Fujimoto, and K. Kawabata, Magnetohydrodynamical processes of the sector structure in the solar wind, *Publ. Astron. Soc. Jap., 22,* 495, 1970.

Hundhausen, A. J., Composition and dynamics of the solar wind plasma, *Rev. Geophys. Space Phys., 8,* 729, 1970.

Hundhausen, A. J., Interplanetary shock waves and the structure of solar wind disturbances, Solar Wind, *NASA Spec. Publ. 308,* p. 393, 1972*a*.

Hundhausen, A. J., *Coronal Expansion and Solar Wind,* Springer, New York, 1972*b*.

Hundhausen, A. J., and R. A. Gentry, Numerical simulation of flare-generated disturbances in the solar wind, *J. Geophys. Res., 74,* 2908, 1969*a*.

Hundhausen, A. J., and R. A. Gentry, The effects of solar flare duration on a double shock pair at 1 AU, *J. Geophys. Res., 74,* 6229, 1969*b*.

Hundhausen, A. J., J. R. Asbridge, S. J. Bame, and I. B. Strong, Vela satellite observations of solar wind ions, *J. Geophys. Res., 72,* 1969, 1967.

Hundhausen, A. J., S. J. Bame, J. R. Asbridge, and S. J. Sydoriak, Solar wind proton properties:

Vela 3 observations from July 1965 to June 1967, *J. Geophys. Res., 75,* 4643, 1970.

Matsuda, T., and T. Sakurai, Dynamics of the azimuthally dependent solar wind, *Cosmic Electrodynamics, 3,* 97, 1972.

Mihalov, J. D., and J. H. Wolfe, Average solar wind properties from Pioneers 6 and 7, *Cosmic Electrodynamics, 2,* 326, 1971.

Ness, N. F., A. J. Hundhausen, and S. J. Bame, Observations of the interplanetary medium: Vela 3 and Imp 3, 1965–1967, *J. Geophys. Res., 76,* 6643, 1971.

Neugebauer, M., and C. W. Snyder, Mariner 2 observations of the solar wind, 1, Average properties, *J. Geophys. Res., 71,* 4469, 1966.

Ogilvie, K. W., Co-rotating shock structures, Solar Wind, *NASA Spec. Publ. 308,* p. 430, 1972.

Parker, E. N., *Interplanetary Dynamical Processes,* Interscience, New York, 1963.

Parker, E. N., Dynamical theory of the solar wind, *Space Sci. Rev., 4,* 666, 1965.

Sarahbai, V., Some consequences of non-uniformity of solar wind velocity, *J. Geophys. Res., 68,* 1555, 1963.

Simon, M., and W. I. Axford, Shock waves in the interplanetary medium, *Planet. Space Sci., 14,* 901, 1966.

Siscoe, G. L., Fluid dynamics of thin solar wind filaments, *Solar Phys., 13,* 490, 1970.

Siscoe, G. L., Structure and orientation of solar wind interaction fronts: Pioneer 6, *J. Geophys. Res., 77,* 27, 1972.

Siscoe, G. L., and L. T. Finley, Meridional (north-south) motions of the solar wind, *Solar Phys., 9,* 452, 1969.

Siscoe, G. L., and L. T. Finley, Solar wind structure determined by corotating coronal inhomogeneities, 1, Velocity-driven perturbations, *J. Geophys. Res., 75,* 1817, 1970.

Siscoe, G. L., and L. T. Finley, Solar wind structure determined by corotating coronal inhomogeneities, 2, Arbitrary perturbations, *J. Geophys. Res., 77,* 35, 1972.

Siscoe, G. L., B. Goldstein, and A. J. Lazarus, An east-west asymmetry in the solar wind velocity, *J. Geophys. Res., 74,* 1759, 1969.

Snyder, C. W., and M. Neugebauer, Interplanetary solar-wind measurements by Mariner 2, *Space Res., 4,* 89, 1964.

Snyder, C. W., M. Neugebauer, and U. R. Rao, The solar wind velocity and its correlation with cosmic-ray variations and with solar and geomagnetic activity, *J. Geophys. Res., 68,* 6361, 1963.

Sonett, C. P., and D. S. Colburn, The SI^+-SI^- pair and interplanetary forward reverse shock ensembles, *Planet. Space Sci., 13,* 675, 1965.

Strong, I. B., J. R. Asbridge, S. J. Bame, H. H. Heckman, and A. J. Hundhausen, Measurements of proton temperatures in the solar wind, *Phys. Rev. Lett., 16,* 631, 1966.

Sturrock, P. A., and J. R. Spreiter, Shock waves in the solar wind and geomagnetic storms, *J. Geophys. Res., 70,* 5345, 1965.

(Received September 22, 1972;
accepted November 16, 1972.)